Vol. 24, No. 3(2025) Alim25633
Revista Mexicana de Ingeniería Química

Calcium carbonate addition decreases the *in vitro* starch digestibility of wheat bread

Adición de carbonato de calcio disminuye la digestibilidad *in vitro* de pan de trigo

L. Acosta-Domínguez[1], R.M. Mata-Ramirez[1], E.J. Vernon-Carter[2], J. Alvarez-Ramirez[2], A. Garcia-Hernandez[1], C.A. Roldan-Cruz[3], S. Garcia-Diaz[4]*

[1]Facultad de Ciencias Químicas. Universidad Veracruzana-Región Xalapa. Gonzalo Aguirre- Beltrán, s/n, Zona Universitaria, Xalapa, Veracruz 91090 México.

[2]División de Ciencias Básicas e Ingeniería. Universidad Autónoma Metropolitana, Unidad Iztapalapa. AP 55-534. Iztapalapa, CDMX, 09340 México.

[3]Facultad de Nutrición. Universidad Veracruzana-Región Veracruz. Calle Carmen Serdán 5, Salvador Díaz Mirón, Veracruz, Veracruz, 91700 México

[4]Facultad de Ciencias Químicas. Universidad Veracruzana-Región Veracruz. Bv. Adolfo Ruíz Cortines 455, Costa Verde, 94294 Veracruz, Ver., México.

Sent date: July 18, 2025; Accepted: October 28, 2025

Abstract

The objective was to prepare white bread with decreased starch digestibility via the incorporation of small amounts of calcium carbonate. The addition of calcium carbonate increased the pH, decreased the titratable acidity and increased the soluble protein content. FTIR analysis showed that calcium carbonate increased the structured water content and modified the protein secondary structure by increasing coils and β-sheet. The short-range ordered and hydrated starch structures determined by FTIR increased, which was seen as indicative of the formation of crosslinked starch networks. The *in vitro* starch digestibility indicated that the calcium carbonate decreased the rapidly digestible and slowly digestible starch fractions by about 33 and 10%, respectively while increasing the resistant starch fraction by about 160% relative to the control bread. Principal component analysis revealed the existent relation between the reduced starch digestibility linked to the formation of ordered starch structures mediated by calcium crosslinking, which limited the binding of amylolytic enzymes to the starch chains.

Keywords: White bread, calcium carbonate, FTIR, *in vitro* digestibility.

Resumen

El objetivo fue preparar pan blanco con digestibilidad de almidón disminuida vía la incorporación de pequeñas cantidades de carbonato de calcio. La adición de carbonato de calcio aumentó el pH, disminuyó la acidez titulable e incrementó el contenido de la proteína soluble. Los análisis FTIR mostraron que el carbonato de calcio aumentó el contenido de agua estructurada y modificó la estructura secundaria de la proteína incrementando las conformaciones de espiral y β-láminas. Asimismo, se incrementaron las estructuras hidratadas y ordenadas a corto alcance del almidón, las cuales fueron vistas como indicativo de la formación de redes de almidón entrecruzadas. La digestibilidad *in vitro* del almidón indicó que el carbonato de calcio disminuyó las fracciones del almidón rápida y lentamente digerible en alrededor de 33 y 10%, respectivamente mientras se aumentaron las fracciones de almidón resistente en alrededor del 160% relativamente al pan control. El análisis de componentes principales reveló la relación existente entre la digestibilidad del almidón ligada a la formación de las estructuras ordenadas de almidón mediado por el entrecruzamiento con el calcio lo cual limitó el enlace de las enzimas amilolíticas con las cadenas de almidón.

Palabras clave: Pan blanco, carbonato de calcio, FTIR, digestibilidad *in vitro*.

*Corresponding author. *E-mail*: samgarcia@uv.mx;
https://doi.org/10.24275/rmiq/Alim25633
ISSN:1665-2738, *issn-e*: 2395-8472

1 Introduction

Bread is considered a staple food highly consumed in the world. Bread production techniques are quite diverse depending on cultural traditions, although all bread recipes comprise cereal flour, water and a leavening agent as the main ingredients (Sluimer, 2005). Bread is a significant source of nutrients for the human diet, providing carbohydrates, proteins and minerals. In particular, the high starch content of bread contributes to the energy requirements for human physical activity. However, excessive consumption of starchy food products combined with a sedentary lifestyle has been linked to unhealthy conditions known as metabolic syndrome (Miao *et al*., 2015). Starch in common white bread can exhibit high digestion rates with the consequent production and absorption of glucose in the small intestine (Meraz *et al*., 2022). Sub-utilized glucose in the blood is transformed and stored in adipose tissue as emulsified lipids, leading eventually to health problems related to metabolic syndrome diseases (Pradham, 2007). In this regard, there is strong motivation to modify the ingredients and methods for bread production to reduce starch digestibility. According to Scazzina *et al*. (2009) sourdough fermented bread gives glycemic responses lower than bread leavened with *S. cerevisiae*. Reshmi et al. (2017) reported that white bread combined with 20% fresh and 5% dry pomelo segments presented higher levels of resistant starch fractions (3.97-10.96%) and low predicted glycemic index (62.97-53.13%). It was postulated that naringin was responsible for the reduced starch digestibility via the inhibition of the binding capacity of hydrolyzing enzymes. Sardabi *et al*. (2021) used Moringa peregrina seed husk as a source of dietary fiber to reduce the starch digestibility in wheat bread. Whitney and Simsek (2017) showed that whole wheat bread exhibited decreased starch digestibility in comparison with white bread. Korompokis *et al*. (2021) determined that the addition of maltogenic amylase decreased the starch digestibility of white bread. Ge *et al*. (2021) showed that bread supplemented with 20% pumpkin flour had reduced starch digestibility by about 55.4% as compared to 69.9% for the non-supplemented bread. The decreased digestibility was explained by the enhanced digesta viscosity by the fiber added and the presence of compact gel networks hindering the contact between starch granules and α-amylase. Bajka *et al*. (2021) found that the incorporation of cellular legume powder can reduce by about 40% the *in vivo* glycemic index without compromising the bread quality. The aforementioned approaches for decreasing starch digestibility rely on the addition of an edible fiber source that acts as an obstruction for amylolytic enzymes. In the present work, we explored the incorporation of calcium carbonate as the calcium source in bread preparation. The hypothesis is that calcium could act as a crosslinking agent of starch chains, promoting the formation of a starch molecular organization that offers increased resistance to the action of amylolytic enzymes and, consequently, decreases starch digestibility. These actions are particularly relevant in the context of addressing metabolic syndrome-related disorders, which represent a growing concern in global nutrition and public health strategies. Calcium is commonly used as a crosslinking agent for biopolymers, including alginate, guar gum and starch (Giz *et al*., 2020; George & Abraham, 2007; Liu *et al*., 2016). Also, calcium has been used as a nutritional additive in bread preparation (Salinas *et al*., 2016; Alsuhaibani, 2018) without appreciable deleterious drawbacks to the sensorial and textural bread characteristics. One expects that the addition of small amounts of calcium carbonate may lead to marked reductions in the enzymatic hydrolysis of bread starch.

2 Materials and methods

2.1 Materials

Commercial wheat flour (Tres Estrellas®, CDMX, Mexico; 73 g carbohydrates, 11 g protein, 1 g lipids, 2 g dietary fiber and 0.0016 g ash per 100 g of flour dry basis), salt, sugar salt, baking dry yeast (TradiPan, CDMX, Mexico) were purchased at a local market (Comercial Mexicana, Veracruz, Mexico). Calcium carbonate used in all experiments were of analytical grade (Sigma-Aldrich, St. Louis, Mo, US).

2.2 Bread preparation

The bread recipe consisted of wheat flour (187.37 g), water (109.42 g), yeast (2.74 g), NaCl (1.82 g), sugar (3.65 g) and $CaCO_3$ (0.0, 0.82, 1.64 or 2.46 g). This study aims to analyze the effect of calcium carbonate on the biopolymers present in bread, considering starch as the primary component affected. Accordingly, the amount of calcium used was calculated based on the starch content. The starch content was estimated by considering starch as the primary carbohydrate in wheat flour. According to the manufacturer, this corresponds to 73 g of starch per 100 g of flour, so that 100 g of starch is equivalent to 136.99 g of wheat flour. The amount of calcium represented 0.0, 0.7, 1.4 and 2.1 g $CaCO_3$/100 g starch. The breads were coded as B_0, B_1, B_2 and B_3, respectively. The preparation of the bread was conducted by mixing the ingredients with the help of a SP-800-J Laboratory Spiral Mixer (Grupo Alpha Simet, Queretaro, Mexico). The wheat flour, yeast, salt, sugar and $CaCO_3$ were put into a mixing bowl and water at 30 °C was added. The ingredients

were mixed at low speed until a homogeneous mix was achieved (5 min). Then the mix was kneaded for 15 min. Subsequently, the mass was transferred to an aluminum mold (20 × 10 × 10 cm) covered with waxed paper and placed in the mechanical convection incubator (BEING Scientific, model BIF-35, Shangai, China) for 2 hours at 35 ºC. Then, the obtained dough was placed in a conventional convection oven (Rational AG, Landsberg, Germany) adjusting temperature at 200º C and 20% relative humidity for 25 minutes. The bread was allowed to reach room temperature and finally stored in hermetic Ziploc bags (4 ºC).

2.3 Methods

Moisture (925.10), ashes (923.03), and titratable acidity (942.15) were analyzed using the official methods instituted by the Association of Official Analytical Chemists (AOAC, 2000). The pH was precise analytically by a digital pH meter (MP220, Mettler, Toledo; AACC method 02-52.01). The soluble protein content was analyzed using the Bradford technique with bovine serum albumin as standard. SEM analysis of the bread crumb was carried out in a JEOL-JMS-7600F microscope with the LM mode at 15 kV accelerating voltage (Akishima, Japan). Samples were fixed on a carbon sample holder with a double-sided sticky tape. were coated in with gold with a thin film sputtering unit (model Desk V, Denton Vacuum) (Ramos-Villacob *et al.*, 2024). Fourier transform infrared (FTIR) spectroscopy was conducted at 20 °C using a equipped FTIR-ATR spectrophotometer (Spectrum 100, Perkin-Elmer, Waltham, MA, USA). All spectra were analyzed following the procedure described by Morales-Huerta *et al.* (2025), using Gaussian and Lorentzian fitting functions implemented in Fortran for spectral deconvolution. *In vitro* starch digestibility was performed with the methodology proposed by Englyst *et al.* (1992). The following discontinuous exponential model was used to explore the presence of multi-phase hydrolysis kinetics (Bello-Perez *et al.*, 2019):

$$X(t) = X_{\infty} + X_{fast}\exp\left(-k_{H,fast}t\right) + X_{slow}\exp\left(-k_{H,slow}t\right) \quad (1)$$

Here, $X(t)$ is the starch concentration at time t, X_{∞} is the residual starch for long times (i.e., indigestible starch), $k_{H,fast}$ and $k_{H,slow}$ are the hydrolysis rate constants for fast and slow kinetics, and X_{fast} and X_{slow} are the concentrations of the fast and slow digestible starch in the initial sample. The model (1) assumed that the starch is composed of three fractions. Two fractions that can be digested, although with different rate, and a third fraction that cannot be hydrolyzed under the amylolytic digestion conditions of the experimental run. For $t = 0$, one has

$$X_0 = X_{\infty} + X_{fast} + X_{slow} \quad (2)$$

This means that the parameters X_{∞}, X_{fast} and X_{slow} are not mutually independent. For a given initial concentration X_0, the parameters of the model (1) were estimated by least-squares fitting of the hydrolysis kinetics data subjected to the constraint (2). The estimation of digestible starch fractions of the bread variations was done as described by Godoy-Ramírez *et al.* (2024); namely, the rapidly digestible starch (RDS) and the slowly digestible starch (SDS) were established as the digested starch after first 20 min and 20-120 min, respectively. Finally, the resistant starch (RS) was taken as the starch that was not digested after 120 min.

2.4 Data analysis

Experimental runs were carried out in triplicate. ANOVA and Tukey's test were conducted with the Statgraphics 7 software (Statistical Graphics Corp. Manugistics Inc., Cambridge, MA). Statistically significance difference was taken when $p<0.05$. A principal component analysis (PCA) was conducted to assess the multi-variate effect of the calcium carbonate in the bread response variables.

3 Results and discussion

The pH of the control white bread without $CaCO_3$ (B_0) was about 5.32, and increased to 6.08, 6.43 and 6.54 for breads B_1, B_2 and B_3 (Table 1). Yeast produced acids during the fermentation process, leading to a slightly acidic medium. Calcium carbonate acted as a neutralizer for the acid medium resulting from the dough leavening.

Table 1. Characteristics of the white bread variations with different calcium content.

Bread	pH	Titratable acidity (%)	Moisture content (%)	Ashes (%)	Soluble protein (%)
B_0	5.32 ± 0.03^{d}	0.42 ± 0.01^{a}	41.37 ± 0.63^{b}	2.66 ± 0.01^{a}	4.34 ± 0.04^{d}
B_1	6.08 ± 0.02^{c}	0.37 ± 0.01^{b}	42.92 ± 0.69^{ab}	2.81 ± 0.02^{b}	8.27 ± 0.05^{c}
B_2	6.43 ± 0.02^{b}	0.35 ± 0.01^{c}	43.88 ± 0.77^{a}	2.93 ± 0.02^{bc}	11.52 ± 0.05^{b}
B_3	6.54 ± 0.02^{a}	0.33 ± 0.01^{d}	43.96 ± 0.77^{a}	2.98 ± 0.02^{c}	12.63 ± 0.05^{a}

Values are reported as means ± standard deviation. Column with different lower-case letters in columns indicate significant differences ($p < 0.05$). B_0 = control; B_1 = 0.7, B_2 = 1.4 and B_3 = 2.1 g $CaCO_3$/100 g starch.

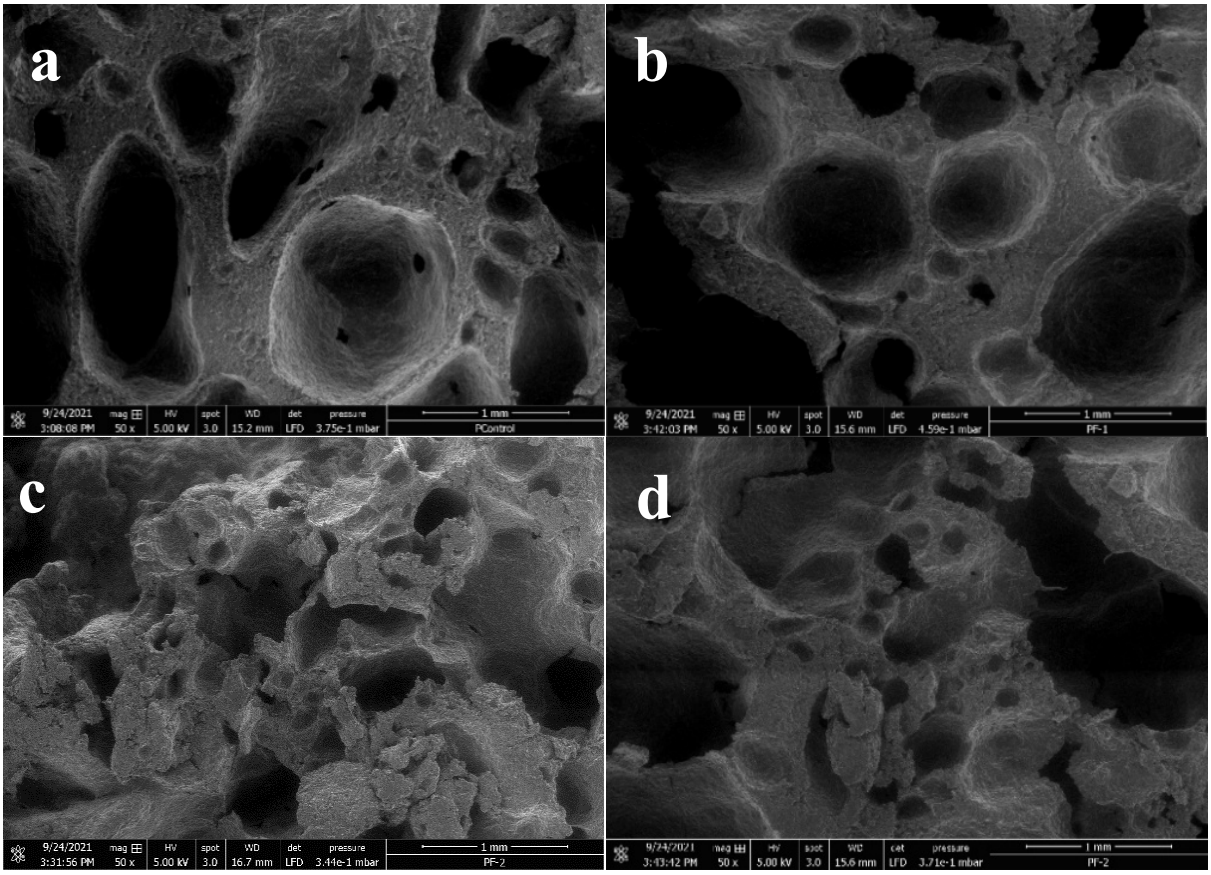

Figure 1. SEM images (50×) from the crumb of the bread variations. a) B_0 = control, b) B_1 = 0.7, c) B_2 = 1.4, d) B_3 = 2.1 g $CaCO_3$/100 g starch.

The effect was also reflected in the titratable acidity, which decreased from about 0.42 mg NaOH 0.1 N/g for B_0 to 0.33 mg NaOH 0.1 N/g for B_3. The moisture content exhibited a slight increase with the calcium carbonate addition, from 41.37% to 43.96 for B_3. Ashes also increased as a consequence of the calcium addition. The most visible variation was exhibited by the soluble protein, which increased from 4.34% for B_0 to 12.63% for B_3. Ono *et al*. (1993) reported that protein solubility increases with the pH, which is in line with the correlation ($\rho = 0.87$) between the pH and protein solubility shown in Table 1.

3.1 Morphology

Figure S1 presents images of bread slices for the control and the bread with the three different levels of calcium carbonate content. The crumb morphology of the control bread (B_0) was homogeneous, and the shape was regular. The calcium carbonate addition produced bread with a heterogeneous distribution of crumb pores and channels. Large pores can be observed in the crumb of B_2 and B_3. Besides, the slice shape was less regular with some fractures discernible in the crust. SEM micrographs offer a more detailed view of the crumb morphology (Figure 1). The high homogeneity of the pore distribution was confirmed for B_0 (Figure 1.a). Starch granules covered by gelatinized starch chains formed a complex 3D network with irregular caves and pores. The sample B_1 exhibited morphology similar to that of the control sample, although with the presence of large fractures (Figure 1.b). The further addition of calcium carbonate produced a less homogeneous crumb morphology (figures 1.c and 1.d) with larger fractures and pores. This suggests that calcium carbonate produced bread with an irregular 3D network formed by starch and proteins. Similar results were found recently by Garcia-Hernandez *et al*. (2022) who reported that baking powder produced less heterogeneous bread morphologies with slightly increased moisture content than bread made with regular yeast as a leavening agent.

3.2 FTIR analysis

Figure 2.a shows the FTIR spectrum of the bread variations in the range 4000-800 cm^{-1} where some salient bands were highlighted. The broad signal at 3600-3000 cm^{-1} corresponds to the hydroxyl group OH linked to the interactions between water and biopolymers (e.g., proteins and starch). The peak at 2950 cm^{-1} is associated to the CH and CH_2 aliphatic

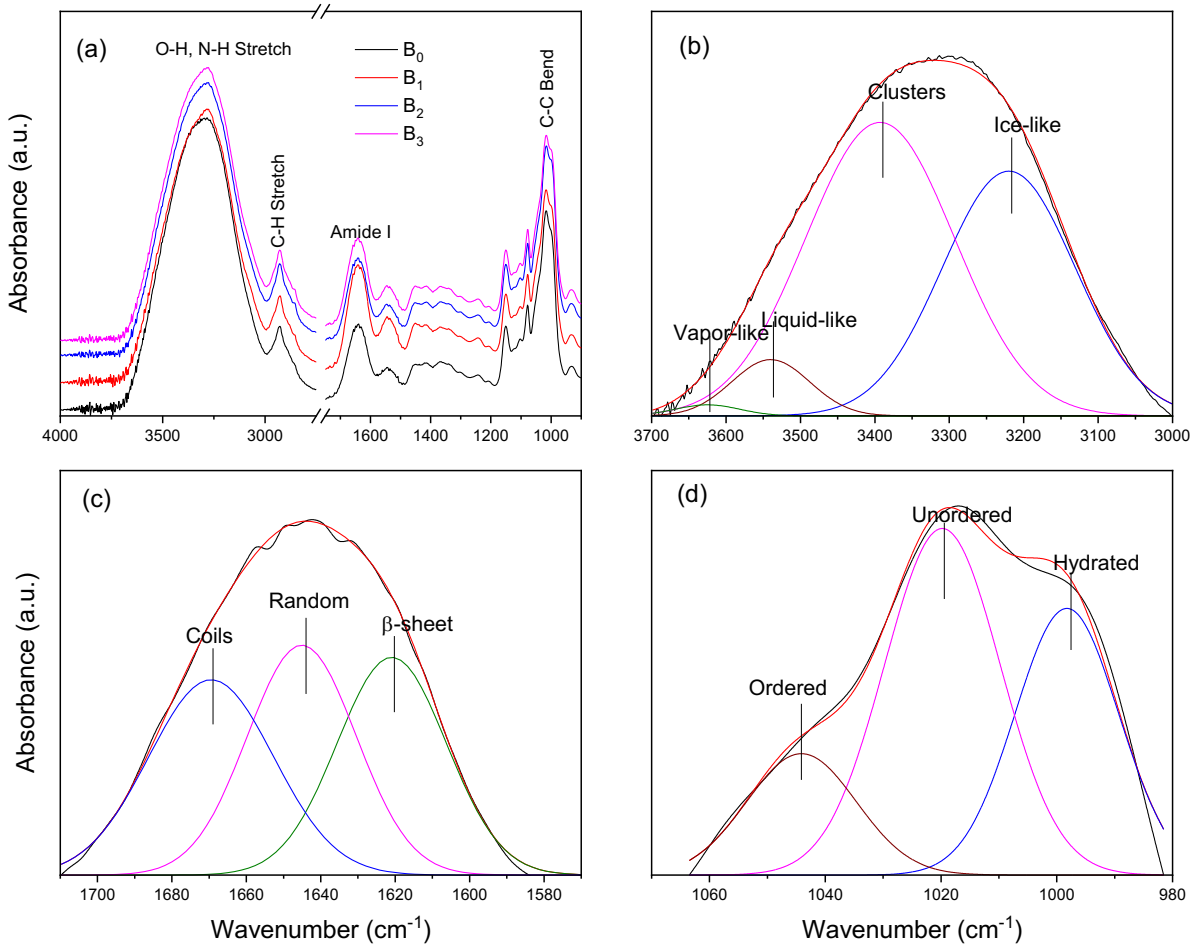

Figure 2. (a) FTIR spectrum for the different bread variations (B_0, B_1, B_2 and B_3). Prominent bands were highlighted, including the OH stretching, the Amide I and the fingerprint starch bands. The subsequent panels illustrate the numerical deconvolution of the FTIR spectrum: (b) the OH stretching band, (c) the Amide I band, and (d) the starch fingerprint region. B_0 = control, B_1 = 0.7, B_2 = 1.4, B_3 = 2.1 g $CaCO_3$/100 g starch.

groups of lipids. The band in the range 1700-1600 cm^{-1} indicate the C=O stretching of the Amide I linked to the bread proteins. The sharp peak at about 1025 cm^{-1} is attributed to the bread carbohydrates, mainly starch.

Figure 2.b shows that the hydroxyl band can be approximated by four Gaussian functions obtained by numerical deconvolution. These findings have been related to the structure of water forming polymeric hydrogels, and can be identified as non-freezing, freezing bound and free water (Vasylieva *et al*., 2018). Free water does not interact with the polymer molecules. Freezing-bound water interacts weakly with biopolymer, and non-freezing-bound water interacts with polymeric chains by forming hydrogen bonds (Goda *et al*., 2006). Water interactions at low wavenumber (i.e., at low-energy levels) reflect strong hydrogen bonds. Water vibrations at high wavenumber (i.e., high-energy levels) can be ascribed to water-water interactions (De Ninno & De Francesco, 2018). Figure S2.b shows that the water structure in the bread is dominated by low-energy vibrations linked to clusters and ice-like structures. Figure 3.a presents the variation of the water structure distribution for the different bread variations. The liquid-like water had significant ($p < 0.05$) variations with the addition of calcium carbonate, which is in line with the small variations of the moisture content shown in Table 1. In contrast, the content of water clusters decreased, and the ice-like water increased with the calcium carbonate content, suggesting that calcium improved the extent of the OH bonds via maybe crosslinking effects. A conceptual illustration of the proposed mechanism is provided in Supplementary Figure S3. Figure 2.c shows that an accurate fitting of the experimental FTIR spectrum in the Amide I region can be achieved by three Gaussian functions. The three individual peaks can be assigned to coils (~1670 cm^{-1}), random (~1642 cm^{-1}) and β-sheets (~1618 cm^{-1}) (Dong *et al*., 1990). These three configurations have a similar relative contribution to the protein secondary structure. Figure 3.b presents the effect of the calcium carbonate on the protein secondary structure of the white bread. Coils decreased with the calcium addition, from about 34% to about 30%. Such decrease was accompanied by an increase in random

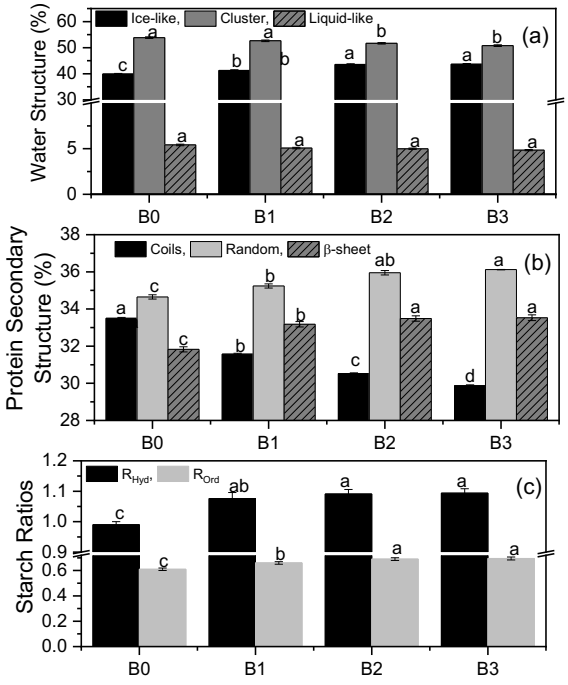

Figure 3. Percentage changes of (a) the water structure components, (b) protein secondary structure and (c) the starch structure ratios for the different bread variations. B_0 = control, B_1 = 0.7, B_2 = 1.4, B_3 = 2.1 g $CaCO_3$/100 g starch. The small letters above bars denote statistically significant differences.

and β-sheet structures. In particular, β-sheets have been linked to the elasticity of gluten, and hence of the wheat dough and bread (Saadi *et al*., 2022).

Figure 2.d shows the graphical deconvolution of the starch backbones in the range 1100-950 cm^1. The spectrum in this region can be approximated by three Gaussian peaks linked to hydrated (~995 cm^{-1}), amorphous (~1022 cm^{-1}) and short-range ordered (~1047 cm^{-1}) starch structures (van Soest *et al*., 1995). Rather than the magnitude of individual peaks, the ratios R_{hyd}=995/1022 and R_{ord}=1047/1022 obtained from the deconvoluted Gaussian function areas are considered to represent the contents of hydrated and short-range ordered structures as compared with amorphous ones. Figure 3.c presents the starch ratios for the different bread formulations. The addition of calcium carbonate led to a significant ($p<0.05$) increase in the FTIR ratios R_{hyd} and R_{ord}. That is, the calcium increased the relative content of the hydrated and short-range ordered starch structures, which can be seen as an insight into the binding of the calcium in the starch chains. It has been postulated that covalent bonds are involved in the calcium-starch interactions (Chatakanonda et al., 2000). FTIR analysis has indicated that linkages are likely to occur between carbons of sugar rings, resulting in the crosslinking of two or more starch chains to give non-regular space networks (Liu et al., 2014). Cornejo-Villegas *et al*. (2018) have postulated that van der Waals interactions might be involved in the interaction of Ca^{2+} ions and starch chains. The increased ratio 1047/1022 is probably indicating the increase of ordering as induced by cross-linking and van der Waals effects.

3.3 In vitro starch digestibility

Figure S2 presents the *in vitro* starch hydrolysis for the control bread (B_0) and the bread added with calcium carbonate (B_1 and B_2). The addition of calcium carbonate decreased the starch hydrolysis after 120 min, from about 95% for B_0 to about 82 and 70% for B_1 and B_2, respectively. The continuous lines in Figure S3 denote the least-squares fitting by Eq. (2) and the estimated parameters are presented in Table 2. It is noted that the transition time t_{tr} is higher than zero, meaning that the digestograms exhibited a two-phase behavior. The first phase for times $t < t_{tr}$ corresponds to a fast hydrolysis rate, and the second phase for times $t > t_{tr}$ corresponds to a slow hydrolysis rate. This transition time increased with the calcium addition, from 16.44 min for B_0 to about 31.98 for B_2. Both the fast and slow hydrolysis rates decreased with the calcium addition. In particular, the fast hydrolysis rate showed a strong decrease from 18.13×10^{-2} 1/min for the control bread B_0 to 3.16×10^{-2} 1/min for B_2. The slow hydrolysis rate showed only a slight decrease with the calcium addition, from 4.37×10^{-2} 1/min for B_0 to 2.91×10^{-2} 1/min for B_2. The decrease in the hydrolysis rate was reflected in the distribution of the digestible starch fractions. The RDS fractions showed a marked decrease from about 25.19% for the control bread B_0 to 17.31% for bread B_2. The SDS fraction showed a similar trend. In contrast, the RS increased from 12.49% for B_0 to about 32.19% for B_2. In this context, certain compounds such as polyphenols may enhance resistant starch (RS) content to a greater extent. Kwaśny *et al*. (2022) reported RS increases exceeding 300 %; however, they also noted that polyphenols can significantly alter the organoleptic properties of food, including color, astringency, and bitterness. Moreover, other compounds are known to promote RS formation, although their effectiveness depends on the type of fiber and the processing conditions applied and (Koksel *et al*., 2025). These results showed that the addition of calcium carbonate had an important impact on starch digestibility by reducing the hydrolysis rate and limiting starch hydrolysis. It was postulated that calcium-mediated cross-linking leads to compact 3D networks, limiting the accessibility of enzymes for binding with starch chains (Roldan-Cruz *et al*., 2020).

Table 2. Estimated parameters of the kinetics model Eq. (1) and the digestible starch fraction according with the classification by Englyst *et al*. (1992).

Bread	$k_{fast} \times 10^2$ (1/min)	$k_{slow} \times 10^2$ (1/min)	RDS (%)	SDS (%)	RS (%)
B_0	1.62 ± 0.05^a	1.57 ± 0.04^a	25.19 ± 1.16^a	62.32 ± 0.63^a	12.49 ± 0.43^d
B_1	1.30 ± 0.02^c	1.24 ± 0.03^b	20.98 ± 0.33^b	57.60 ± 0.69^b	21.42 ± 0.69^c
B_2	1.46 ± 0.02^c	0.79 ± 0.02^c	17.31 ± 0.24^c	51.50 ± 0.77^c	31.19 ± 0.77^b
B_3	1.61 ± 0.03^b	0.71 ± 0.02^c	16.51 ± 0.17^c	48.12 ± 0.64^{cd}	35.37 ± 0.77^a

Values are reported as means ± standard deviation. Column with different lower-case letters in columns indicate significant differences ($p < 0.05$). B_0 = control, B_1 = 0.7, B_2 = 1.4 and B_3 = 2.1 g $CaCO_3$/100 g starch.

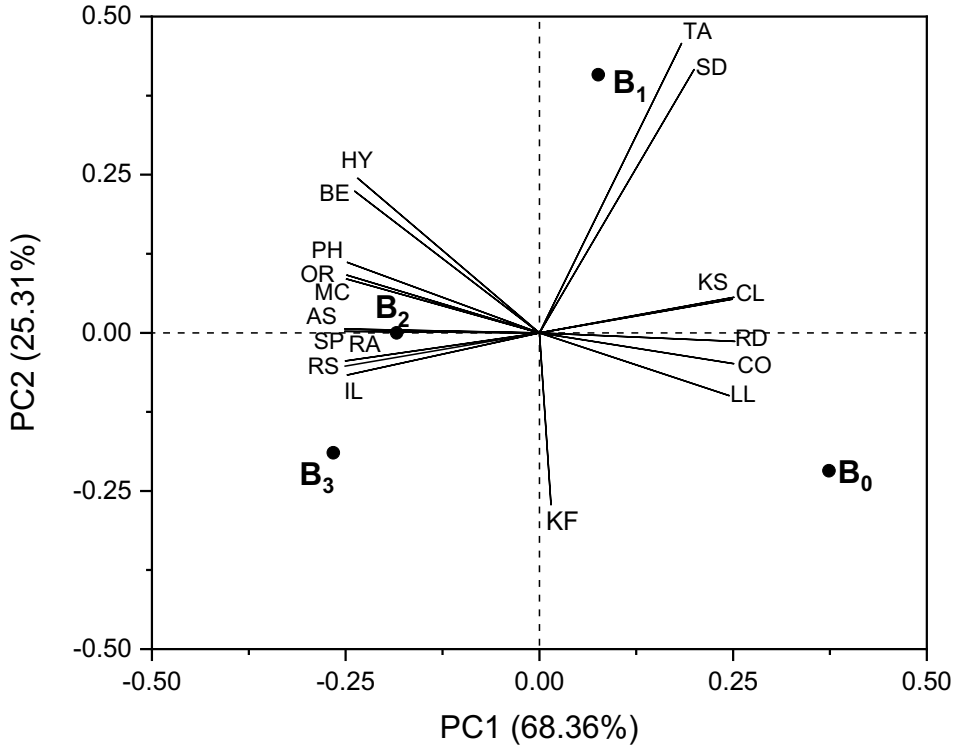

Figure 4. Bi-plot of the principal component analysis (PCA) results for the 19 response variables of the three bread variations. B_0 = control; B_1 = 0.7; B_2 = 1.4, B_3 = 2.1 g $CaCO_3$/100 g starch.

3.4 Principal component analysis (PCA)

The following set of 19 response variables was considered for PCA: pH (PH), moisture content (MC), titratable acidity (TA), ashes (AS), soluble protein (SP), ice-like (IL), clusters (CL), liquid-like (LL) water structures, coils (CO), random (RA) and β-sheet (BE) protein structures, hydrated R_{hyd} (HY) and short-range ordered R_{ord} (SO) starch structures, fast hydrolysis rate (KF), slow hydrolysis rate (KS), RDS (RD), SDS (SD) and RS (RS). The letters in parenthesis correspond to the acronyms used for denoting the response variables in a score bi-plot (Figure 4). The first and second principal components accounted for 68.36 and 25.31% of the total variability. The response variables were aggregated about two clusters, with one in the negative part of PC1 and the other in the positive part of PC1. The RDS and SDS fractions are aligned with the hydrolysis rates (KS and KF), and also with the titratable acidity (TA). This is not surprising since acids contribute to the hydrolysis of the starch chains. Interestingly, the RS fraction is aligned with the transition time (TT) from fast to slow hydrolysis rate, the pH, the soluble protein (SP), and the hydrated (HY) and short-range ordered (OR) starch structures. The alignment with SP might be indicating that soluble protein promoted the formation of complexes with the starch chains, decreasing in this the ability of the amylolytic enzymes to breakdown the starch chains. Lin *et al*. (2020) showed that proteins promote the formation of ordered starch structures that mitigate starch digestibility. The increase of starch ordered structures was reflected by the 1047/1022 FTIR ratio R_{ord}. The protein secondary structure (CO, RA and BE) and the water structure (IL, CL and LL) showed poor

alignment with the starch digestibility, suggesting that the water and protein structures played only a minor role in the *in vitro* digestibility of the bread starch.

Conclusions

This work studied the effect of adding calcium carbonate in the *in vitro* starch digestibility of white bread. The main conclusion is that small amounts of calcium carbonate addition to wheat bread led to a marked decrease in the *in vitro* starch digestibility. The effect was ascribed to the formation of a starch network mediated by calcium-mediated cross-linking, which limits the action of amylolytic enzymes. Calcium carbonate addition is a simple, viable and inexpensive technique to obtain white bread with reduced starch digestibility.

References

AACC International. Approved Methods of Analysis. Method 02-52.01. Hydrogen-Ion Activity (pH). Method 44-15.02. Electrometric Method; St. Paul, MN, U.S.A., 999.

Alsuhaibani, A. (2018). Rheological and nutritional properties and sensory evaluation of bread fortified with natural sources of calcium. *Journal of Food Quality*, 2018, 8308361. https://doi.org/10.1155/2018/8308361

AOAC (2000) *Official Methods of Analysis*. 17th Edition. The Association of Official Analytical Chemists, Gaithersburg, MD, USA.

Bajka, B. H., Pinto, A. M., Ahn-Jarvis, *et al*. (2021). The impact of replacing wheat flour with cellular legume powder on starch bioaccessibility, glycaemic response and bread roll quality: A double-blind randomised controlled trial in healthy participants. *Food Hydrocolloids*, 114, 106565. https://doi.org/10.1016/j.foodhyd.2020.106565

Bello-Perez, L. A., Agama-Acevedo, E., Garcia-Valle, D. E., & Alvarez-Ramirez, J. (2019). A multiscale kinetics model for the analysis of starch amylolysis. *International journal of biological macromolecules*, 122, 405-409. http://doi.org/10.1016/j.ijbiomac.2018.10.161

Chatakanonda, P., Varavinit, S. & Chinachoti, P. (2000). Effect of crosslinking on thermal and microscopic transitions of rice starch. *LWT-Food Science and Technology*, 33, 276-284. https://doi.org/10.1006/fstl.2000.0662

Cornejo-Villegas, M. D. L. Á., Rincón-Londoño, N., Real-López, D. & Rodríguez-García, M. E. (2018). Effect of Ca^{2+} ions on the pasting, morphological, structural, vibrational, and mechanical properties of corn starch–water system. *Journal of Cereal Science*, 79, 174-182. https://doi.org/10.1016/j.jcs.2017.10.003

De Ninno, A. & De Francesco, M. (2018). ATR-FTIR study of the isosbestic point in water solution of electrolytes. *Chemical Physics*, 513, 266-272. https://doi.org/10.1016/j.chemphys.2018.08.018

Dong, A., Huang, P. & Caughey, W. S. (1990). Protein secondary structures in water from second-derivative amide I infrared spectra. *Biochemistry*, 29, 3303-3308. https://doi.org/10.1021/bi00465a022

Englyst, H. N., Kingman, S. M. & Cummings, J. H. (1992). Classification and measurement of nutritionally important starch fractions. *European Journal of Clinical Nutrition*, 46, S33-50. PMID: 1330528

Garcia-Hernandez, A., Roldan-Cruz, C., Vernon-Carter, E. J. & Alvarez-Ramirez, J. (2022). Effects of leavening agent and time on bread texture and *in vitro* starch digestibility. *Journal of Food Science and Technology*, 59, 1922-1930. https://doi.org/10.1007/s13197-021-05206-1

Ge, F., Wu, P. & Chen, X. D. (2021). Evolutions of rheology, microstructure and starch hydrolysis of pumpkin-enriched bread during simulated gastrointestinal digestion. *International Journal of Food Science & Technology*, 56, 6000-6010. https://doi.org/10.1111/ijfs.15273

George, M. & Abraham, T. E. (2007). pH sensitive alginate–guar gum hydrogel for the controlled delivery of protein drugs. *International Journal of Pharmaceutics*, 335, 123-129. https://doi.org/10.1016/j.ijpharm.2006.11.009

Giz, A. S., Berberoglu, M., Bener, S., Aydelik-Ayazoglu, S., Bayraktar, H., Alaca, B. E., & Catalgil-Giz, H. (2020). A detailed investigation of the effect of calcium crosslinking and glycerol plasticizing on the physical properties of alginate films. *International Journal of Biological Macromolecules*, 148, 49-55. https://doi.org/10.1016/j.ijbiomac.2020.01.103

Goda, T., Watanabe, J., Takai, M. & Ishihara, K. (2006). Water structure and improved mechanical properties of phospholipid polymer hydrogel with phosphorylcholine centered intermolecular cross-linker. *Polymer*, 47, 1390-1396. https://doi.org/10.1016/j.polymer.2005.12.04

Godoy-Ramírez, A., Rodríguez-Huezo, M. E., Lara-Corona, V.H., Vernon_Carter, E.J., & Alvarez-Ramirez, J. (2024). Wheat bread supplemented with potato peel flour: color, molecular organization, texture. *Revista Mexicana de Ingeniería Química*, 23, Alim24201. https://doi.org/10.24275/rmiq/Alim24201

Koksel, H., Samray, M. N., Masatcioglu, T. M., & Koksel, F. (2025). Quality of resistant starch-enriched breadcrumbs extrudates. *Cereal Chemistry*, *102*(2), 364-376. https://doi.org/10.1002/cche.10863

Kwaśny, D., Borczak, B., Sikora, M., & Kapusta-Duch, J. (2022). Preliminary study on the influence of the polyphenols of different groups on the digestibility of wheat starch, measured by the content of resistant starch. *Applied Sciences*, *12*(21), 10859. https://doi.org/10.3390/app122110859

Korompokis, K., Deleu, L. J., De Brier, N. & Delcour, J. A. (2021). Investigation of starch functionality and digestibility in white wheat bread produced from a recipe containing added maltogenic amylase or amylomaltase. *Food Chemistry*, 362, 130203. https://doi.org/10.1016/j.foodchem.2021.130203

Lin, L., Yang, H., Chi, C. & Ma, X. (2020). Effect of protein types on structure and digestibility of starch-protein-lipids complexes. *LWT*, 134, 110175. https://doi.org/10.1016/j.lwt.2020.110175

Liu, H., Guan, Y., Wei, D., Gao, C., Yang, H. & Yang, L. (2016). Reinforcement of injectable calcium phosphate cement by gelatinized starches. *Journal of Biomedical Materials Research Part B: Applied Biomaterials*, 104, 615-625. https://doi.org/10.1002/jbm.b.33434

Liu, J., Wang, B., Lin, L., Zhang, J., Liu, W., Xie, J. & Ding, Y. (2014). Functional, physicochemical properties and structure of cross-linked oxidized maize starch. *Food Hydrocolloids*, 36, 45-52. https://doi.org/10.1016/j.foodhyd.2013.08.013

Meraz, M., Vernon-Carter, E. J., Bello-Perez, L. A. & Alvarez-Ramirez, J. (2022). Mathematical modeling of gastrointestinal starch digestion-blood glucose-insulin interactions. *Biomedical Signal Processing and Control*, 77, 103812. https://doi.org/10.1016/j.bspc.2022.103812

Miao, M., Jiang, B., Cui, S. W., Zhang, T. & Jin, Z. (2015). Slowly digestible starch—A review. *Critical Reviews in Food Science and Nutrition*, 55, 1642-1657. https://doi.org/10.1080/10408398.2012.704434

Morales-Huerta, A., Vernon-Carter, E. J., Alvarez-Ramirez, J., & Román-Guerrero, A. (2025). Effect of microwave dry-heat treatment of wheat flour in the *in vitro* digestibility of bread starch. *International Journal of Biological Macromolecules*, 144392. https://doi.org/10.1016/j.ijbiomac.2025.144392

Ono, T., Katho, S. & Mothizuki, K. (1993). Influences of calcium and pH on protein solubility in soybean milk. *Bioscience, Biotechnology, and Biochemistry*, 57, 24-28. https://doi.org/10.1271/bbb.57.24

Pradhan, A. (2007). Obesity, metabolic syndrome, and type 2 diabetes: inflammatory basis of glucose metabolic disorders. *Nutrition Reviews*, 65(suppl_3), S152-S156. https://doi.org/10.1111/j.1753-4887.2007.tb00354.x

Ramos-Villacob, V., Figueroa-Flórez, J. G., Salcedo-Mendoza, J. E., Hernández-Ruidíaz, J. E., Romero-Verbel, L. A. (2024). Development of modified cassava starches by ultrasound-assisted amylose/lauric acid. *Revista Mexicana de Ingeniería Química*, 23, Alim24109.

https://doi.org/10.24275/rmiq/Alim24109

Reshmi, S. K., Sudha, M. L. & Shashirekha, M. N. (2017). Starch digestibility and predicted glycemic index in the bread fortified with pomelo (Citrus maxima) fruit segments. *Food Chemistry*, 237, 957-965. https://doi.org/10.1016/j.foodchem.2017.05.138

Roldan-Cruz, C., Garcia-Diaz, S., Garcia-Hernandez, A., Alvarez-Ramirez, J. & Vernon-Carter, E. J. (2020). Microstructural changes and *in vitro* digestibility of maize starch treated with different calcium compounds used in nixtamalization processes. *Starch - Stärke*, 72, 1900303. https://doi.org/10.1002/star.201900303

Saadi, S., Saari, N., Ghazali, H. M., Abdulkarim, S. M., Hamid, A. A. & Anwar, F. (2022). Gluten proteins: Enzymatic modification, functional and therapeutic properties. *Journal of Proteomics*, 251, 104395. https://doi.org/10.1016/j.jprot.2021.104395

Salinas, M. V., Zuleta, A., Ronayne, P. & Puppo, M. C. (2016). Wheat bread enriched with organic calcium salts and inulin. A bread quality study. *Journal of Food Science and Technology*, 53, 491-500. https://doi.org/10.1007/s13197-015-2008-8

Sardabi, F., Azizi, M. H., Gavlighi, H. A. & Rashidinejad, A. (2021). The effect of Moringa peregrina seed husk on the *in vitro* starch digestibility, microstructure, and quality of white wheat bread. *LWT*, 136, 110332. https://doi.org/10.1016/j.lwt.2020.110332

Scazzina, F., Del Rio, D., Pellegrini, N. & Brighenti, F. (2009). Sourdough bread: Starch digestibility and postprandial glycemic response. *Journal of Cereal Science*, 49, 419-421. https://doi.org/10.1016/j.jcs.2008.12.008

Sluimer, P., 2005. *Principles of Breadmaking: Functionality of Raw Materials and Process Steps*. American Association of Cereal Chemists, St. Paul.

Whitney, K. & Simsek, S. (2017). Reduced gelatinization, hydrolysis, and digestibility in whole wheat bread in comparison to white bread. *Cereal Chemistry*, 94, 991-1000. https://doi.org/10.1094/CCHEM-05-17-0116-R

van Soest, J. J., Tournois, H., de Wit, D. & Vliegenthart, J. F. (1995). Short-range structure in (partially) crystalline potato starch determined with attenuated total reflectance Fourier-transform IR spectroscopy. *Carbohydrate Research*, 279, 201-214. https://doi.org/10.1016/0008-6215(95)00270-7

Vasylieva, A., Doroshenko, I., Vaskivskyi, Y., Chernolevska, Y. & Pogorelov, V. (2018). FTIR study of condensed water structure. *Journal of Molecular Structure*, 1167, 232-238. https://doi.org/10.1016/j.molstruc.2018.05.002